

Available online at www.sciencedirect.com

Polyhedron 27 (2008) 1343–1352



POLYHEDRON

www.elsevier.com/locate/poly

Synthesis, structure, DNA binding and oxidative cleavage activity of ternary (L-leucine/isoleucine) copper(II) complexes of heterocyclic bases

Ramakrishna Rao^a, Ashis K. Patra^b, P.R. Chetana^{a,*}

^a Department of Chemistry, Central College, Bangalore University, Bangalore 560 001, India

^b Department of Inorganic and Physical Chemistry, Indian Institute of Science, Sir C.V. Raman Avenue, Bangalore 560 012, India

Received 17 October 2007; accepted 24 December 2007

Available online 4 March 2008

Abstract

Six ternary α -amino acid copper(II) complexes of the general formula $[\text{Cu}(\text{AA})(\text{B})(\text{H}_2\text{O})](\text{X})$ (**1–6**), where AA is L-leu = L-leucine (**1–3**) or L-ile = L-isoleucine (**4–6**), B is a *N,N*-donor heterocyclic base, viz. 2,2'-bipyridine (bpy, **1, 4**), 1,10-phenanthroline (phen, **2, 5**) and dipyrrodo[3,2:2',3'-f]quinoxaline (dpq, **3, 6**) and $\text{X} = \text{ClO}_4^-/\text{NO}_3^-$ have been synthesized, characterized, and their DNA binding and cleavage activity studied. The bpy and dpq complexes of L-ile (**4, 6**) have been structurally characterized by X-ray crystallography. The complexes show a distorted square-pyramidal (4 + 1) CuN_3O_2 coordination geometry. The one-electron paramagnetic complexes display a d–d band near 600 nm in water and show a cyclic voltammetric response due to a Cu(II)/Cu(I) couple near -0.1 V (vs. SCE) in DMF-0.1 M TBAP. All complexes are 1:1 electrolytes. Binding interactions of the complexes with calf thymus DNA (CT-DNA) have been investigated by absorption, emission, viscosity and DNA melting studies. The phen and dpq complexes are avid binders to the calf thymus DNA, giving an order: (**3, 6**) (dpq) > (**2, 5**) (phen) \gg (**1, 4**) (bpy). The bpy complexes do not show any apparent binding to the DNA and hence show poor DNA cleavage activity. The phen and dpq complexes (**2, 3, 5, 6**) show efficient oxidative cleavage of pUC19 supercoiled DNA (SC-DNA) in the presence of the reducing agent 3-mercaptopropionic acid (MPA) involving hydroxyl radical ($\cdot\text{OH}$) species, as evidenced from the control data showing inhibition of DNA cleavage in the presence of $\cdot\text{OH}$ radical quenchers, viz. DMSO, mannitol, KI and catalase.

© 2008 Elsevier Ltd. All rights reserved.

Keywords: Copper; DNA binding; DNA cleavage; Crystal structure; L-Leucine; L-Isoleucine; Phenanthroline base

1. Introduction

The development of compounds cleaving DNA under physiological conditions, i.e. ‘artificial nucleases’, are of current interest for their potential applications in genomic research and as footprinting and therapeutic agents [1–10]. The ability to accomplish site-specific DNA cleavage will undoubtedly allow the development of new chemotherapeutic agents and antimicrobial drugs. In addition, artificial nucleases will provide important new tools for DNA manipulation to molecular biologists. For example, bis-

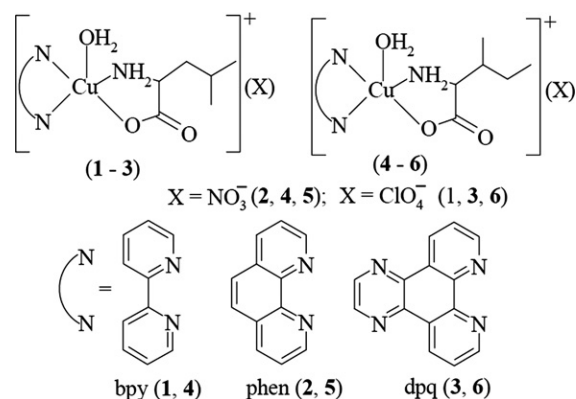
phenanthroline copper(I) complex is used in DNA-footprinting experiments [1], which are important for the detailed study of DNA–protein interactions [7a]. 3d transition metal complexes are well suited for application as artificial nucleases, because of their cationic nature, diverse three-dimensional structural features depending on the ligand systems, and the possibility to tune their redox potential through the choice of proper ligands. The interaction of transition metals like Mn, Fe and Cu, with dioxygen in the presence of a reducing agent generates reactive oxygen species (ROS) that ultimately may cleave DNA [7b]. The DNA cleavage could occur by two major pathways, viz. hydrolytic and oxidative pathway. Hydrolytic DNA cleavage involves cleavage of the phosphodiester bond to

* Corresponding author. Tel.: +91 80 22961353; fax: +91 80 22386988.
E-mail address: pr.chetana@gmail.com (P.R. Chetana).

generate fragments those could be subsequently relegated. Zn(II), being a strong Lewis acid, exchanges ligands very rapidly. Several Zn(II) complexes are well-known for their hydrolase activity [7c]. Hydrolytic cleavage active species mimic restriction enzymes. The oxidative DNA cleavage involves either oxidation of the deoxyribose moiety by abstraction of sugar hydrogen or oxidation of nucleobases. Oxidative DNA cleavage by redox-active metal complexes, like $[\text{Fe}(\text{edta})]^{2-}$ or $\text{Cu}(\text{1,10-phenanthroline})_2\text{Cl}_2$, is mediated by the production of reactive oxygen species, like HO^\bullet , through a Fenton-type mechanism [10]. These free radicals abstract the most accessible and exposed sugar hydrogens and initiate the oxidative cleavage, leading to DNA-cleavage products. The purine base guanine is most susceptible for oxidation among the four nucleobases. The role of ternary copper(II) complexes in biological systems is well known [11]. Among the transition metal based DNA cleaving agents, copper phenanthroline complexes are particularly primarily sugar directed. They are responsible for direct strand scission by hydrogen atom abstraction from the deoxyribose moiety. Sigman and coworkers have reported that the bis-(1,10-phenanthroline)copper(I) complex in the presence of H_2O_2 act as a ‘chemical nuclease’ that efficiently nicks DNA [1,2]. Recently there have been several reports of copper(II) complexes showing efficient chemical nuclease activity [12–17]. Recent reports have shown that amino acid/peptide based copper(II) complexes show efficient DNA cleavage activity by oxidative and hydrolytic pathways [17–22]. Such complexes may show DNA cleavage both in the presence (chemical nuclease) or absence (hydrolytic) of a reducing agent. The favored pathway depends on several factors, viz. Lewis acidity, accessible redox potential and rate of ligand exchange.

The present work stems from our interest to explore the structural and functional properties of redox active ternary copper(II) complexes having bioessential α -amino acids L-leucine or L-isoleucine and *N,N*-donor heterocyclic bases as a DNA groove binder. The efficiency of the DNA strand scission can be enhanced by increasing the binding affinity of the metal complex for DNA. Typically such coordination complexes contain a DNA-binding moiety that binds either at a groove, or act as an intercalator, thereby increasing the DNA-targeting ability of the metal complex. Our choice of 2,2'-bipyridine (bpy), 1,10-phenanthroline (phen) and dipyridoquinoxaline (dpq) are based on their differences in DNA binding ability. Both L-leucine and L-isoleucine are essential for development of skeletal muscle tissue and preserve muscle glycogen levels [24].

Herein, we report the syntheses, structure, DNA binding and oxidative DNA cleavage properties of ternary copper(II) complexes of the general formula $[\text{Cu}(\text{L-leu/ile})(\text{B})(\text{H}_2\text{O})](\text{X})$ (1–6) where B is a *N,N*-donor heterocyclic base, viz. 2,2'-bipyridine (bpy, 1, 4); 1,10-phenanthroline (phen, 2, 5) and dipyrido[3,2-*d*:2',3'-*f*]quinoxaline (dpq, 3, 6), L-leu = L-leucine and L-ile = L-isoleucine (Scheme 1). The bpy and dpq complexes of L-ile (4, 6) have been struc-



Scheme 1. Complexes 1–6 and the heterocyclic bases.

turally characterized by X-ray crystallography. Studies have been made to explore the role of DNA binder and amino acid along with mechanistic pathways involved in the ‘chemical nuclease’ activity.

2. Experimental

2.1. Materials

All products were obtained from commercial sources and were used without further purification. Solvents used for electrochemical and spectroscopic studies were purified by standard procedures [25]. The supercoiled pUC19 DNA (CsCl purified) was purchased from Bangalore Genei (India). Calf thymus (CT) DNA, agarose (molecular biology grade), distamycin-A, catalase, superoxide dismutase (SOD) and ethidium bromide (EB) were obtained from Sigma (USA). Tris(hydroxymethyl)aminomethane-HCl (Tris-HCl) buffer solution was prepared by using deionized, sonicated triple distilled water. The *N,N*-donor heterocyclic base dipyrido[3,2-*d*:2',3'-*f*]quinoxaline (dpq) was prepared by the literature procedure using 1,10-phenanthroline-5,6-dione as a precursor and reacting it with ethylenediamine [26]. The complexes 2 and 5 were prepared by literature procedures [27].

2.2. Preparation of $[\text{Cu}(\text{AA})(\text{B})(\text{H}_2\text{O})](\text{X})$ (1–6) (AA = L-leu (1–3) or L-ile (4–6); B = bpy, phen, dpq); X = NO_3^- (2, 4, 5); ClO_4^- (1, 3, 6)

The complexes were prepared by following a modified reported [27] synthetic procedure in which a 10 ml aqueous solution of $\text{Cu}(\text{NO}_3)_2 \cdot 3\text{H}_2\text{O}$ (0.48 g) or $\text{Cu}(\text{ClO}_4) \cdot 6\text{H}_2\text{O}$ (0.75 g) (2.0 mmol) was reacted with L-leucine or L-isoleucine (0.27 g, 2.1 mmol) treated with NaOH (0.08 g, 2.0 mmol) in water (10 ml) under magnetic stirring at room temperature. Slow evaporation of the solution at room temperature yielded a crystalline material. Crystals of complexes 4 and 6 were suitable for X-ray diffraction studies. After 30 min, a 20 ml methanolic solution of the heterocyclic base [bpy (0.28 g), phen (0.35 g), dpq (0.42 g) (1.8 mmol)] was added to the solution and the resulting

mixture was stirred for 2 h at room temperature. On cooling the solution to an ambient temperature, it was filtered and the filtrate on slow concentration yielded a crystalline solid of the product. The solid was isolated and washed with cold aqueous methanol and finally dried over P_4O_{10} (Yield: $\sim 75\%$). *Anal. Calc.* for $C_{16}H_{22}CuN_3O_7Cl$ (**1**): C, 41.12; H, 4.74; N, 8.99. Found: C, 41.32; H, 4.88; N, 8.85%. λ_{max} , nm (ϵ , $M^{-1} cm^{-1}$) in water: 604 (50), 310 (12560), 300 (12700), 242 (10,020). FT-IR, cm^{-1} (KBr disc): 3486br, 3340br, 3092m, 2953m, 2873w, 1633s, 1606s, 1498m, 1474m, 1446m, 1385s, 1316m, 1250m, 1110vs (ClO_4^-), 1067s, 976m, 833m, 770s, 731m, 652w, 620m, 553m, 416m (s, strong; m, medium; w, weak; br, broad; vs, very strong). A_M ($\Omega^{-1} cm^2 M^{-1}$) in water at 25 °C: 104. μ_{eff} (solid, 298 K): $1.78 \mu_B$. *Anal. Calc.* for $C_{18}H_{22}CuN_4O_6$ (**2**): C, 47.61; H, 4.88; N, 12.34. Found: C, 47.35; H, 4.47; N, 12.18%. λ_{max} , nm (ϵ , $M^{-1} cm^{-1}$) in water: 610 (55), 293 (9,640), 272 (31380), 204 (43860). FT-IR, cm^{-1} (KBr disc): 3385br, 3219br, 2953m, 1634s, 1585s, 1520m, 1430s, 1384vs (NO_3^-), 1315s, 1154m, 1130w, 1109w, 1041m, 984m, 918w, 857s, 826m, 782m, 723s, 649m, 559m, 429m. A_M ($\Omega^{-1} cm^2 M^{-1}$) in water at 25 °C: 122. μ_{eff} (solid, 298 K): $1.74 \mu_B$. *Anal. Calc.* for $C_{20}H_{22}CuN_5O_7Cl$ (**3**): C, 44.20; H, 4.08; N, 12.89. Found: C, 44.13; H, 4.03; N, 12.78%. λ_{max} , nm (ϵ , $M^{-1} cm^{-1}$) in water: 608 (74), 293 (15000), 257 (47600), 208 (31540). FT-IR, cm^{-1} (KBr disc): 3499br, 3293br, 2957m, 1594s, 1531w, 1486s, 1470m, 1407s, 1386s, 1215m, 1114s, 1084vs (ClO_4^-), 879w, 824m, 732s, 625s, 576m, 438m. A_M ($\Omega^{-1} cm^2 M^{-1}$) in water at 25 °C: 115. μ_{eff} (solid, 298 K): $1.76 \mu_B$. *Anal. Calc.* for $C_{16}H_{22}CuN_4O_6$ (**4**): C, 44.68; H, 5.16; N, 13.03. Found: C, 44.56; H, 5.20; N, 12.78%. λ_{max} , nm (ϵ , $M^{-1} cm^{-1}$) in water: 604 (55), 310 (13420), 300 (13620), 243 (10220). FT-IR, cm^{-1} (KBr disc): 3500br, 3287br, 3026m, 2959m, 2875m, 1654s, 1601s, 1497m, 1479m, 1383vs (NO_3^-), 1255m, 1159s, 1134m, 1086m, 1063m, 1033m, 1019m, 989m, 897m, 825w, 806w, 774s, 731s, 662w, 584w, 417m. A_M ($\Omega^{-1} cm^2 M^{-1}$) in water at 25 °C: 138. *Anal. Calc.* for $C_{18}H_{22}CuN_4O_6$ (**5**): C, 47.61; H, 4.88; N, 12.34. Found: C, 47.43; H, 4.53; N, 12.43%. λ_{max} , nm (ϵ , $M^{-1} cm^{-1}$) in water: 611 (55), 293 (8320), 272 (27620), 204 (38660). FT-IR, cm^{-1} (KBr disc): 3444br, 3252br, 3133m, 3056w, 2956m, 2874m, 1644s, 1586m, 1518m, 1432m, 1382vs (NO_3^-), 1332m, 1225w, 1158m, 1108w, 1007m, 873w, 856s, 825m, 781m, 737w, 723s, 648m, 567m, 489w, 429m. A_M ($\Omega^{-1} cm^2 M^{-1}$) in water at 25 °C: 127. μ_{eff} (solid, 298 K): $1.80 \mu_B$. *Anal. Calc.* for $C_{20}H_{22}CuN_5O_7Cl$ (**6**): C, 44.20; H, 4.08; N, 12.89. Found: C, 44.33; H, 4.05; N, 12.93%. λ_{max} , nm (ϵ , $M^{-1} cm^{-1}$) in water: 609 (80), 295 (14400), 257 (45840), 208 (26260). FT-IR, cm^{-1} (KBr disc): 3433br, 3286br, 3086m, 2961m, 1637s, 1582m, 1532m, 1487s, 1460m, 1407s, 1387s, 1213m, 1087vs (ClO_4^-), 873m, 823m, 733s, 625s, 568m, 431m. A_M ($\Omega^{-1} cm^2 M^{-1}$) in water at 25 °C: 106. μ_{eff} (solid, 298 K): $1.77 \mu_B$.

Solubility and stability. The complexes showed high solubility in water, methanol, dimethylformamide (DMF) and

dimethyl sulfoxide (DMSO) and are insoluble in hydrocarbons. They are stable in the solid and in solution phases.

Caution! Perchlorate salts are potentially explosive and only small quantities were handled with care.

2.3. General methods

The elemental analysis was done using a Thermo Finnigan FLASH EA 1112 CHNS analyzer. The infrared and electronic spectra were recorded on Perkin–Elmer Lambda 35 and Perkin–Elmer spectrum one 55 spectrophotometers, respectively. DNA melting experiments were carried out on a Varian Cary 300 Bio UV–Vis spectrophotometer attached to a Cary Peltier temperature controller. Molar conductivity measurements were done using a Control Dynamics (India) conductivity meter. Electrochemical measurements were made at 25 °C on an EG&G PAR model 253 VersaStat potentiostat/galvanostat with electrochemical analysis software 270 using a three electrode setup consisting of a glassy carbon working, platinum wire auxiliary and a saturated calomel reference electrode (SCE) in DMF containing 0.1 M TBAP. The electrochemical data were uncorrected for junction potentials. Magnetic susceptibility data at 298 K were obtained using Model 300 Lewis-coil-force magnetometer of George Associates Inc. (Berkley, USA) make.

2.4. X-ray crystallographic procedures

Single crystals of $[Cu(L-ile)(bpy)(H_2O)](NO_3) \cdot H_2O$ (**4** · H_2O) and $[Cu(L-ile)(dpq)(H_2O)](ClO_4)$ (**6**) were obtained by slow evaporation of an aqueous-methanolic solution of the complexes. A rectangular single crystal was mounted on a glass fiber and used for data collection. All geometric and intensity data were collected at 293 K using an automated Bruker SMART APEX CCD diffractometer equipped with a fine focus 1.75 kW sealed tube Mo $K\alpha$ X-ray source ($\lambda = 0.71073 \text{ \AA}$), with increasing ω (width of $0.3^\circ/\text{frame}$) at a scan speed of 5 and 2 s/frame for complexes **4** and **6**, respectively. Intensity data, collected using the $\omega-2\theta$ scan mode, were corrected for Lorentz-polarization effects and for absorption [28]. SMART software was used for data acquisition and SAINT software for data extraction [29]. Absorption corrections were made using SADABS [30]. The structures were solved and refined by the full-matrix least-squares method using the SHELX system of programs [31]. All non-hydrogen atoms were refined anisotropically. All hydrogen atoms attached to the heteroatoms were in their calculated positions and refined using a riding model. Perspective views of the complexes were obtained by ORTEP [32].

2.5. DNA binding experiments

The UV absorbance at 260 and 280 nm of the CT-DNA solution in 5 mM Tris–HCl buffer (pH 7.2) gave a ratio of 1.9, indicating the DNA was free of protein [33]. The

concentration of CT DNA was measured from the band intensity at 260 nm with a known ϵ value ($6600 \text{ M}^{-1} \text{ cm}^{-1}$) [34]. Absorption titration measurements were done by varying the concentration of CT DNA, keeping the metal complex concentration constant in 5 mM Tris–HCl/5 mM NaCl buffer (pH 7.2). Samples were kept for equilibrium before recording each spectrum. The intrinsic binding constant (K_b) for the interaction of the complexes with CT-DNA were determined from a plot of $[\text{DNA}]/(\epsilon_a - \epsilon_f)$ vs. $[\text{DNA}]$ using absorption spectral titration data and the following equation:

$$[\text{DNA}]/(\epsilon_a - \epsilon_f) = [\text{DNA}]/(\epsilon_b - \epsilon_f) + [K_b(\epsilon_b - \epsilon_f)]^{-1},$$

where $[\text{DNA}]$ is the concentration of DNA in base pairs. The apparent absorption coefficients ϵ_a , ϵ_f and ϵ_b correspond to $A_{\text{obsd}}/[\text{Cu}]$, the extinction coefficient for the free copper(II) complex and extinction coefficient for the copper(II) complex in the fully bound form, respectively [35]. K_b is given by the ratio of the slope to the intercept.

The apparent binding constant (K_{app}) values of the complexes were determined by a fluorescence spectral technique using ethidium bromide (EB) bound CT DNA solution in Tris–HCl/NaCl buffer (pH, 7.2). The emission intensities of EB at 600 nm (546 nm excitation) with an increasing amount of the ternary complex concentration were recorded. Ethidium bromide was non-emissive in Tris–buffer medium due to fluorescence quenching of the free EB by the solvent molecules [36]. In the presence of DNA, EB showed enhanced emission intensity due to its intercalative binding to DNA. A competitive binding of the copper complexes to CT DNA could result in the displacement of EB or quenching of the bound EB by the paramagnetic copper(II) species, decreasing its emission intensity.

DNA-melting experiments were carried out by monitoring the absorbance of CT-DNA (200 μM NP) at 260 nm with varying temperature in the absence and presence of the complexes in a 2:1 ratio of DNA to complex with a ramp rate of $0.5 \text{ }^\circ\text{C min}^{-1}$ in phosphate buffer (pH 6.85) using a Peltier system attached to the UV–Vis spectrophotometer.

Viscometric titrations were performed with a Schott Gerate AVS 310 Automated Viscometer. The viscometer was thermostated at $37 \text{ }^\circ\text{C}$ in a constant temperature bath. The concentration of DNA was 200 μM in NP and the flow times were measured with an automated timer, each sample was measured three times and an average flow time was calculated. Data were presented as $(\eta/\eta_0)^{1/3}$ vs. $[\text{complex}]/[\text{DNA}]$, where η is the viscosity of DNA in the presence of complex and η_0 was the viscosity of DNA alone. Viscosity values were calculated from the observed flowing time of DNA-containing solutions (t) corrected for that of buffer alone (t_0), $\eta = (t - t_0)$ [37].

2.6. DNA cleavage experiments

The extent of cleavage of supercoiled (SC) DNA in the presence of the complex and reducing agent MPA was determined by agarose gel electrophoresis. In a typical

reaction, supercoiled pUC19 DNA (0.2 μg), taken in 50 mM Tris–HCl buffer (pH 7.2) containing 50 mM NaCl, was treated with the complex. The extent of cleavage was measured from the intensities of the bands using the UVI-TEC Gel Documentation System.

For mechanistic investigations, inhibition reactions were carried out by adding the reagents prior to the addition of the complex. The solutions were incubated for 1 h in a dark chamber at $37 \text{ }^\circ\text{C}$, followed by addition to the loading buffer containing 25% bromophenol blue, 0.25% xylene cyanol and 30% glycerol (2 μL), and the solution was finally loaded on 1.0% agarose gel containing 1.0 $\mu\text{g/ml}$ ethidium bromide (EB). Electrophoresis was carried out for 2 h at 60 V in tris–acetate–EDTA (TAE) buffer. Bands were visualized by UV light and photographed for analysis. Due corrections were made to the observed intensities for the low level of NC form present in the original sample of SC DNA and for the low affinity of EB binding to SC in comparison to nicked circular (NC) and linear forms of DNA [38]. The concentration of the complexes or the additives mentioned corresponded to the quantity of the sample in 2 μL stock solution prior to dilution to the 20 μL final volume by Tris–HCl buffer.

3. Results and discussion

3.1. Synthesis and general aspects

The ternary copper(II) complexes are prepared in high yield from the reaction of $\text{Cu}(\text{NO}_3)_2 \cdot 3\text{H}_2\text{O}$ or $\text{Cu}(\text{ClO}_4)_2 \cdot 6\text{H}_2\text{O}$ with L-leucine/L-isoleucine and heterocyclic bases. The complexes are stable and soluble in water and common polar organic solvents. They are characterized from the analytical and physicochemical data (Table 1). The complexes display an intense charge transfer (CT) band in the range 200–310 nm, that can be attributed to the $\pi \rightarrow \pi^*$ transition of the coordinated *N,N*-donor heterocyclic base. The d–d band is observed at ~ 600 nm in aqueous medium and is in agreement with a square-pyramidal geometry (Fig. 1). The complexes are redox active and display a cyclic voltammetric response near -0.1 V vs. SCE in DMF-0.1 M TBAP. The redox process is assignable to the Cu(II)/Cu(I) couple. The complexes show 1:1 electrolytic behavior in solution.

3.2. Crystal structures

The bpy and dpq complexes of L-isoleucine (**4** · H_2O , **6**) are structurally characterized using the single-crystal X-ray diffraction technique. Selected crystallographic data are summarized in Table 2. The ORTEP views of the complexes are shown in Figs. 2 and 3. Selected bond distances and angles are given in Table 3. The crystal structures of $[\text{Cu}(\text{L-leu})(\text{phen})(\text{H}_2\text{O})](\text{NO}_3)$ (**2**) and $[\text{Cu}(\text{L-ile})(\text{phen})(\text{H}_2\text{O})](\text{NO}_3)$ (**5**) are known [27]. Both the complexes show distorted (4 + 1) square-pyramidal geometry, in which Cu^{2+} coordinates with two nitrogen atoms of 1,10-phenanthroline, the amino nitrogen atom and one carboxylate oxygen atom of

Table 1
Physicochemical data for the ternary copper(II) complexes 1–6

Complex	1	2	3	4	5	6
IR ^a : [$\nu(\text{NO}_3^-/\text{ClO}_4^-)/\text{cm}^{-1}$]	1110 (ClO_4^-)	1384 (NO_3^-)	1084 (ClO_4^-)	1383 (NO_3^-)	1382 (NO_3^-)	1087 (ClO_4^-)
d–d band: $\lambda_{\text{max}}/\text{nm}$ ($\epsilon/\text{M}^{-1} \text{cm}^{-1}$) ^b	604 (50)	610 (55)	608 (74)	604 (55)	611 (55)	609 (80)
CV: $E_{1/2}/\text{V}$ ($\Delta E_p/\text{mV}$) ^c	–0.13 (430)	–0.10 (330)	–0.06 (390)	–0.13 (440)	–0.12 (340)	–0.10 (360)
A_M^d ($\Omega^{-1} \text{cm}^2 \text{M}^{-1}$)	104	122	115	138	127	106
K_a^e (M^{-1})	1.06×10^4	4.66×10^5	1.15×10^6	1.66×10^4	5.75×10^5	9.8×10^5
K_b^f (M^{-1})		5.1×10^3	1.05×10^4		2.24×10^3	1.92×10^4
ΔT_m^g ($^\circ\text{C}$)	1.0 (± 0.2)	2.4 (± 0.2)	3.2 (± 0.2)	1.3 (± 0.3)	2.7 (± 0.2)	3.0 (± 0.3)

^a KBr phase.

^b In aqueous medium.

^c Cu(II)/Cu(I) couple in DMF–0.1 M TBAP. $E_{1/2} = 0.5(E_{\text{pa}} + E_{\text{pc}})$, $\Delta E_p = |E_{\text{pa}} - E_{\text{pc}}|$, where E_{pa} and E_{pc} are the anodic and cathodic peak potentials, respectively. Scan rate: 50 mV s⁻¹.

^d In aqueous medium at 25 $^\circ\text{C}$.

^e Apparent DNA binding constant from competitive binding assay by the emission method.

^f Intrinsic DNA binding constant (K_b) from the absorption spectral method.

^g Changes in melting temperature of CT DNA.

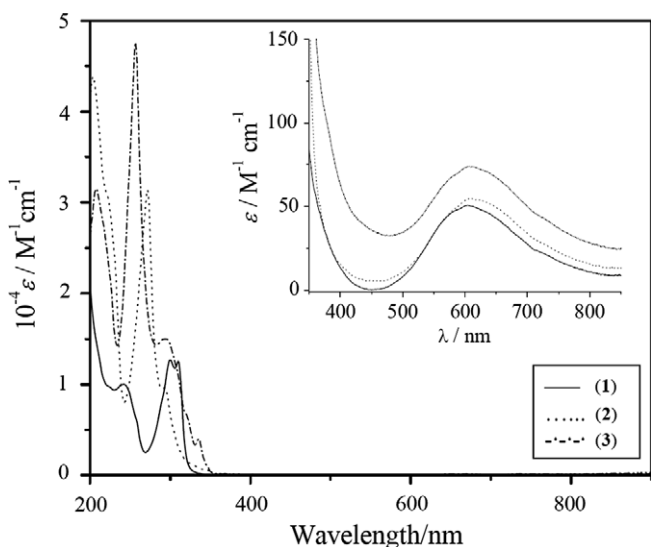


Fig. 1. Electronic spectra of complexes 1 (—), 2 (···) and 3 (– · – ·) in water. The inset shows the d–d band of complexes 1–3.

L-Leu/Ile in equatorial positions, and an oxygen atom of water in the elongated axial position. Complexes 4 and 6 crystallize in the non-centrosymmetric $P2_1$ (monoclinic) and $P1$ (triclinic) space groups, having one and two independent molecules in the crystallographic asymmetric unit respectively. The copper(II) ion is coordinated in a distorted square-pyramidal (4 + 1) coordination geometry through the carboxylate oxygen atom O(1) and the amino nitrogen atom N(3) of L-isoleucine and two N-atoms of 2,2'-bipyridine/dpq and a weakly bound apical water molecule (average trigonal distortion parameter, τ ($4 \cdot \text{H}_2\text{O}$) = 0.268; τ_{av} (6) = 0.087) [39]. Both the structures resemble the corresponding known structure of $[\text{Cu}(\text{L-leu/L-ile})(\text{phen})(\text{H}_2\text{O})](\text{NO}_3)$ [27]. The configuration at the isoleucine chiral α -carbon is S in both complexes. The copper atom is displaced by ~ 0.15 and ~ 0.19 \AA from the mean plane through its basal atoms in the direction towards the apical water molecule for complexes 4 and 6, respectively.

Table 2
Selected crystallographic data for $4 \cdot \text{H}_2\text{O}$ and 6

	$4 \cdot \text{H}_2\text{O}$	6
Formula	$\text{C}_{16}\text{H}_{24}\text{CuN}_4\text{O}_7$	$\text{C}_{20}\text{H}_{22}\text{ClCuN}_5\text{O}_7$
Crystal size (mm)	$0.26 \times 0.18 \times 0.12$	$0.65 \times 0.30 \times 0.20$
Formula weight (g M^{-1})	447.93	543.42
Crystal system	monoclinic	triclinic
Space group (no.)	$P2_1$ (no. 4)	$P1$ (no. 1)
a (\AA)	11.559(4)	8.2524(19)
b (\AA)	6.659(2)	11.940(3)
c (\AA)	13.226(5)	13.440(3)
α ($^\circ$)	90.0	109.257(4)
β ($^\circ$)	92.777(6)	101.000(4)
γ ($^\circ$)	90.0	106.193(4)
V (\AA^3)	1016.8(6)	1140.7(5)
Z	2	2
T (K)	293(2)	293(2)
D_{calc} (g cm^{-3})	1.463	1.582
λ (\AA) (Mo K α)	0.71073	0.71073
Absorption coefficient (cm^{-1})	11.18	11.27
Data/restraints/parameters	3885/1/253	8546/3/613
Goodness-of-fit on F^2	1.130	1.025
R (F_o) ^a [$I > 2\sigma(I)$] (R [all data])	0.0404 (0.0448)	0.0547 (0.0882)
wR (F_o) ^b [$I > 2\sigma(I)$] (wR [all data])	0.1138 (0.1166)	0.1198 (0.1378)
Largest difference in peak and hole (e \AA^{-3})	0.679 and –0.266	0.485 and –0.273
$w = 1/[\sigma^2(F_o^2) + (AP)^2 + (BP)]$	$A = 0.0595$; $B = 0.1680$	$A = 0.0640$; $B = 0.0000$

^a $R = \sum ||F_o| - |F_c|| / \sum |F_o|$.

^b $wR = \{ \sum [w(F_o^2 - F_c^2)^2] / \sum [w(F_o^2)^2] \}^{1/2}$; $w = [\sigma^2(F_o^2) + (AP)^2 + BP]^{-1}$, $P = (F_o^2 + 2F_c^2)/3$.

Both the bpy (4) and dpq (6) structures show extensive intermolecular non-covalent interactions. While one hydrogen atom of the axial water ligand is hydrogen-bonded to the carboxylate oxygen atom belonging to the neighbouring molecule (distances: 2.678 and 2.819 \AA), the other hydrogen atom is H-bonded with the oxygen atom of the lattice $\text{NO}_3^-/\text{ClO}_4^-$ anion (distances: 2.776 and 2.851 \AA). The unit cell packing diagrams and intermolecular hydrogen bonding interactions present in $4 \cdot \text{H}_2\text{O}$ and 6 are shown in Figs. S1–S4 (see supporting information).

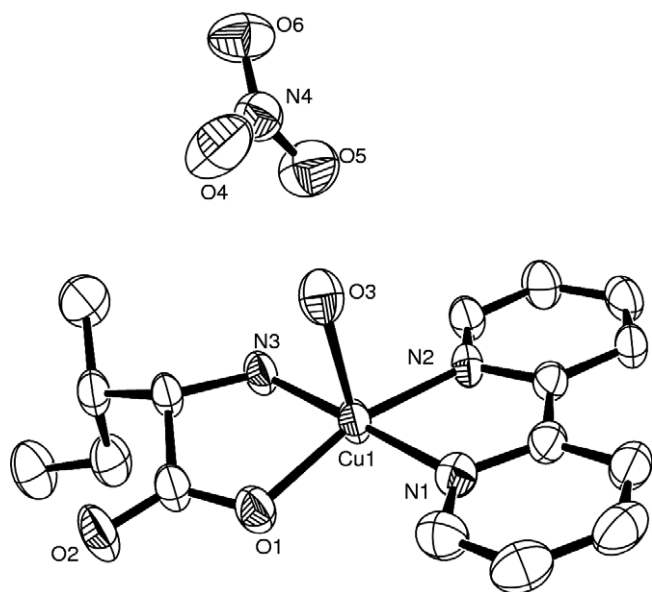


Fig. 2. ORTEP diagram of complex **4** showing 50% probability thermal ellipsoids with the atom labelling scheme for the metal and heteroatoms.

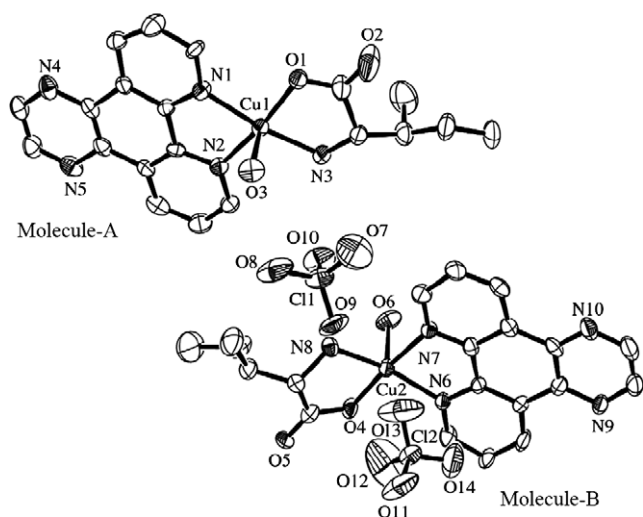


Fig. 3. ORTEP diagram of two independent molecules of complex **6** showing 30% probability thermal ellipsoids with the atom labelling scheme for the metal and heteroatoms.

3.3. DNA binding properties

The binding of complexes **1–6** to calf thymus (CT) DNA has been studied by electronic absorption spectral techniques. The interaction of complex **5** with DNA had been reported earlier [27d]. We have studied this complex for comparison with the other analogous complexes here. The absorption spectral traces of complex **3** with increasing concentration of CT DNA are shown in Fig. 4. We have observed a minor bathochromic shift of ~ 3 nm along with significant hypochromicity for the phen and dpq complexes. The intrinsic DNA binding constants (K_b) of the complexes to CT DNA are obtained by monitoring the

change of the absorption intensity of the spectral bands with increasing concentration of CT DNA, keeping the complex concentration constant. The bpy complexes show weak binding to the DNA due to less extended planarity compared to phen or dpq, which is consistent with the observed trend in hypochromism. The K_b values for complexes **2** and **3** are 5.1×10^3 and $1.05 \times 10^4 \text{ M}^{-1}$, respectively. The higher binding propensity of the phen and dpq complexes in comparison to their bpy analogues could be due to the presence of extended planar aromatic rings facilitating non-covalent interactions with the DNA molecule. Earlier studies on bis-phen copper complex have shown that this complex binds to DNA either by partial intercalation or by binding of one phen ligand to the minor groove while the other phen making favourable contacts within the groove [40–43]. The nature of binding of the phen complex is proposed to be similar as observed for the bis-phen species.

The emission spectral method is used to study the relative binding of the complexes to calf thymus-DNA. The emission intensity of ethidium bromide (EB) is used as a spectral probe as EB shows no apparent emission intensity in buffer solution because of solvent quenching and shows an enhancement of the emission intensity when intercalatively bound to DNA [44]. The binding of the complexes to DNA decreases the emission intensity of EB. The relative binding propensity of the complexes to DNA is measured from the extent of reduction of the emission intensity (Fig. 5, Table 1). The reduction of the emission intensity of EB on increasing the complex concentration could be caused due to displacement of the DNA bound EB by the ternary copper(II) complexes.

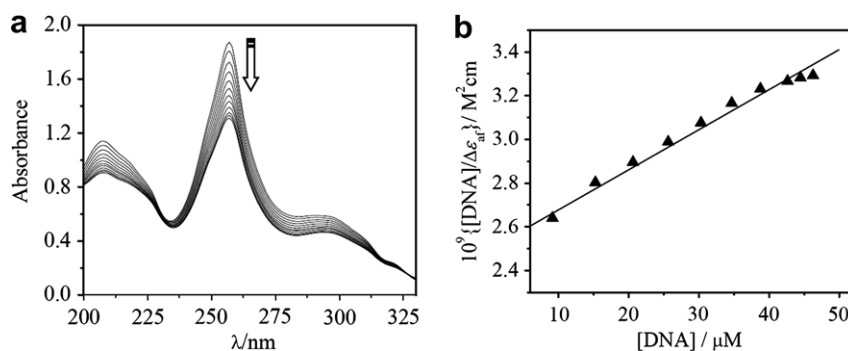
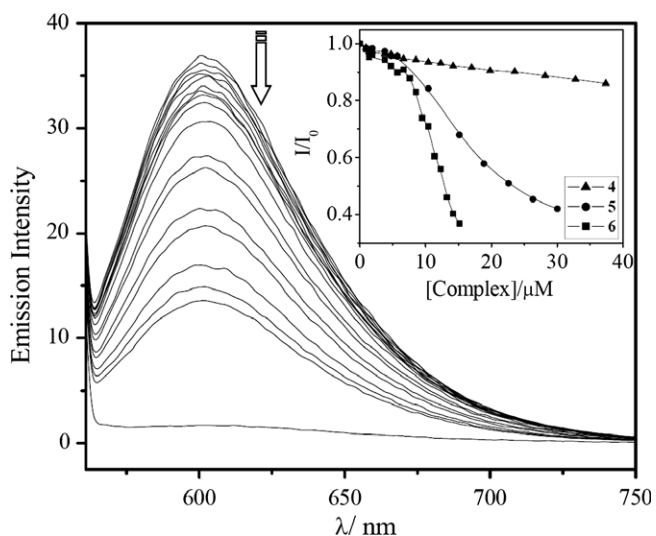
The denaturation of DNA from double-strand to single strand results in absorption hyperchromism at 260 nm. The binding of metal complexes to the double-stranded DNA usually stabilizes the duplex structure to some extent, depending on the strength of the interaction with the nucleic acid [45]. The binding should lead to an increase in the melting temperature (T_m) of DNA as compared to DNA itself. The binding of the phen and dpq complexes results in a moderate increase (~ 2 °C) in the melting temperatures (ΔT_m) of CT-DNA suggesting primarily an electrostatic and/or groove binding nature of the complexes (Table 1, Fig. 6a).

To investigate further the binding modes of the complexes viscosity measurements on solutions of calf thymus DNA incubated with the complexes were carried out. Because the viscosity of a DNA solution is sensitive to the addition of organic drugs and metal complexes bound by intercalation, we examined the effect on the specific relative viscosity of DNA upon addition of complexes. The relative specific viscosity (η/η_0), (η and η_0 are the specific viscosities of DNA in the presence and absence of a complex, respectively) of DNA reflects the increase in contour length associated with the separation of DNA base pairs caused by intercalation. The relative viscosity of DNA and contour length follows the equation: $(\eta/\eta_0) = (L/L_0)^{1/3}$,

Table 3

Selected bond distances (Å) and angles (°) for $[\text{Cu}(\text{L-ile})(\text{bpy})(\text{H}_2\text{O})](\text{NO}_3) \cdot \text{H}_2\text{O}$ (**4** · H_2O) and for the two molecules of $[\text{Cu}(\text{L-ile})(\text{dpq})(\text{H}_2\text{O})](\text{ClO}_4)$ (**6**)

4 · H_2O	6				
	Molecule A			Molecule B	
Cu(1)–N(1)	1.991(3)	1.997(7)	Cu(2)–N(6)	2.023(7)	
Cu(1)–N(2)	2.014(3)	2.013(7)	Cu(2)–N(7)	2.014(6)	
Cu(1)–N(3)	1.972(3)	2.008(7)	Cu(2)–N(8)	1.978(7)	
Cu(1)–O(1)	1.930(3)	1.953(6)	Cu(2)–O(4)	1.894(6)	
Cu(1)–O(3)	2.297(3)	2.281(6)	Cu(2)–O(6)	2.294(7)	
N(1)–Cu(1)–N(2)	81.11(13)	81.8(3)	N(6)–Cu(2)–N(7)	82.3(3)	
N(1)–Cu(1)–N(3)	179.24(13)	169.5(3)	N(6)–Cu(2)–N(8)	163.0(3)	
N(1)–Cu(1)–O(1)	95.09(12)	92.8(3)	N(6)–Cu(2)–O(4)	94.3(3)	
N(1)–Cu(1)–O(3)	90.22(13)	95.0(3)	N(6)–Cu(2)–O(6)	99.2(3)	
N(2)–Cu(1)–N(3)	99.59(12)	100.2(3)	N(7)–Cu(2)–N(8)	97.6(3)	
N(2)–Cu(1)–O(1)	163.10(15)	170.1(3)	N(7)–Cu(2)–O(4)	172.9(3)	
N(2)–Cu(1)–O(3)	97.78(14)	96.2(3)	N(7)–Cu(2)–O(6)	91.7(3)	
N(3)–Cu(1)–O(1)	84.15(12)	83.7(3)	N(8)–Cu(2)–O(4)	83.9(3)	
N(3)–Cu(1)–O(3)	90.00(14)	94.9(3)	N(8)–Cu(2)–O(6)	97.9(3)	
O(1)–Cu(1)–O(3)	98.69(12)	92.5(3)	O(4)–Cu(2)–O(6)	95.0(3)	

Fig. 4. (a) Absorption spectral traces on addition of CT DNA to a solution of **3** (shown by arrow). (b) Plot of $[\text{DNA}]/(\epsilon_a - \epsilon_f)$ vs. $[\text{DNA}]$ for the absorption titration of CT-DNA with complex **3**.Fig. 5. Emission spectral changes on addition of $[\text{Cu}(\text{L-ile})(\text{dpq})(\text{H}_2\text{O})](\text{ClO}_4)$ (**6**) to CT-DNA bound to ethidium bromide (shown by arrow). Inset: Effect of addition of $[\text{Cu}(\text{L-ile})(\text{B})(\text{H}_2\text{O})](\text{X})$ [**B** = bpy (**4**, ▲); phen (**5**, ●); dpq (**6**, ■)] to the emission intensity CT DNA-bound ethidium bromide in a 5 mM Tris–HCl/5 mM NaCl buffer (pH 7.2) at 25 °C.

where L and L_0 are the contour length of DNA in the presence and absence of complex respectively [37]. A classical intercalator such as EtBr could cause a significant increase in the viscosity of DNA solutions, in contrast, a partial and/or non-classical intercalation of the ligand could bend or kink DNA resulting in a decrease in its effective length with a concomitant increase in its viscosity [46,47]. The plots of relative viscosities with $R = [\text{Cu}]/[\text{DNA}]$ are shown in Fig. 6(b). The change in relative viscosity for the dpq complexes are more than that for the phen or bpy analogues suggesting greater DNA binding propensity of the dpq complexes in comparison to the phen or bpy analogues, but this change is less compared to that of potential classical intercalators, e.g. ethidium bromide. This is consistent with the observed trend shown by other optical methods and suggests primarily an electrostatic and/or groove binding nature of the complex.

3.4. DNA cleavage studies

The oxidative DNA cleavage activity of the complexes in the presence of the reducing agent 3-mercaptopropionic acid (MPA, 5 mM) was studied by agarose gel electrophoresis

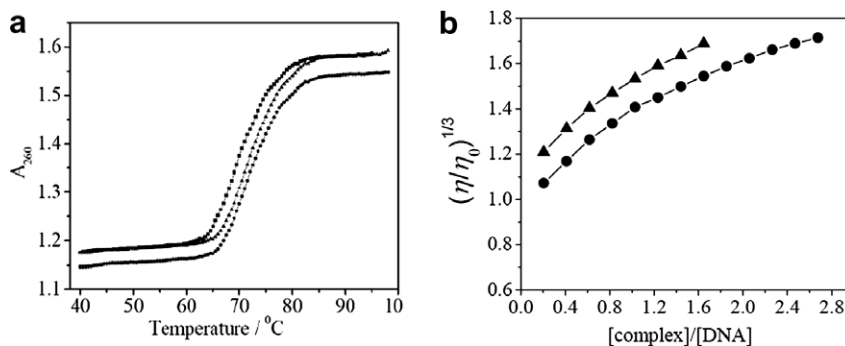


Fig. 6. (a) Effect of addition of complexes **3** (●) and **6** (▲) (50 μM) on the melting temperature of CT-DNA (■) (200 μM) in 5 mM Phosphate buffer (pH 6.85) with a ramp rate of 0.5 °C/min. (b) Change in relative specific viscosity of CT-DNA (150 μM) with addition complexes **2** (●) and **3** (▲) in 5 mM Tris-Cl buffer medium at 37 ± 0.1 °C.

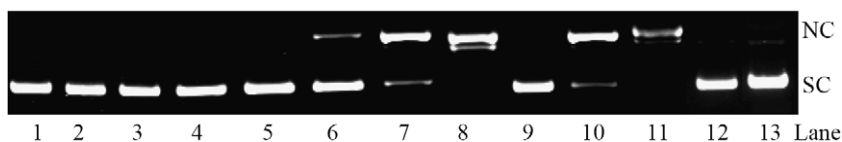


Fig. 7. Gel electrophoresis diagram showing the cleavage of SC pUC19 DNA (0.2 μg, 30 μM) by complexes **1–6** (30 μM) in 50 mM Tris-HCl/50 mM NaCl buffer (pH 7.2) in the presence of MPA (5 mM): Lane 1, DNA + MPA; Lane 2, DNA + L-leu (30 μM) + MPA; Lane 3, DNA + L-ile (30 μM) + MPA; Lane 4, DNA + **2**; Lane 5, DNA + **5** + MPA; Lane 6, DNA + **1** + MPA; Lane 7, DNA + **2** + MPA; Lane 8, DNA + **3** + MPA; Lane 9, DNA + **4** + MPA; Lane 10, DNA + **5**; Lane 11, DNA + **6** + MPA; Lane 12, DNA + distamycin-A (100 μM) + **2** + MPA; Lane 13, DNA + distamycin-A (100 μM) + **6** + MPA.

using supercoiled (SC) plasmid pUC19 DNA (0.2 μg, 30 μM NP) in 50 mM Tris-HCl/50 mM NaCl buffer (pH, 7.2) and the copper(II) complexes (Fig. 7). Selected DNA cleavage data are given in Table 4. The phen and dpq complexes show significant “chemical nuclease” activity. 30 μM of complexes **3** and **6** show almost complete conversion of the SC (form I) to its nicked circular form (NC, form II) of DNA. Control experiments using only MPA or the ternary complexes alone do not show any apparent conversion of SC to its nicked-circular (NC) form. The DNA cleavage activity order for the complexes follows the relative binding propensities of the complexes to DNA. The bpy complexes are cleavage inactive due to their poor binding ability to ds-DNA. This may be attributed to ROS forms which may not be able to reach the SC-DNA by diffusion and consequently are quenched by solvent molecules. To determine the groove binding preference of the complexes, control experiments have been carried out in the presence of the minor groove binder distamycin-A [48]. Inhibition of cleavage in the presence of distamycin-A for both the phen and dpq complexes suggest their minor groove binding nature.

Mechanistic aspects of the chemical nuclease reactions were investigated using various control experiments (Fig. 8). The addition of hydroxyl radical scavengers, [49] like DMSO, catalase and KI, shows significant inhibition of the DNA cleavage activity of the complexes, indicating the possibility of the involvement of the hydroxyl radical and/or a “copper-oxo” intermediate as the reactive species. Addition of superoxide dismutase (SOD) does not show any apparent effect on the DNA cleavage activity, suggesting the non-involvement of $O_2^{\cdot-}$ in the cleavage reaction

Table 4

Selected cleavage data of SC pUC19 (0.2 μg, 30 μM NP) by complexes **1–6**^a

Sl. no	Reaction condition	[Complex]/ μM	% SC	% NC
1	DNA + MPA		97	3
2	DNA + L-leucine (30 μM) + MPA		95	5
3	DNA + L-isoleucine (30 μM) + MPA		96	4
4	DNA + 2	30	92	8
5	DNA + 5	30	94	6
6	DNA + 1 + MPA	30	86	14
7	DNA + 2 + MPA	30	24	76
8	DNA + 3 + MPA	30	10	90 ^b
9	DNA + 4 + MPA	30	88	12
10	DNA + 5 + MPA	30	28	72
11	DNA + 6 + MPA	30	11	89 ^b
12	DNA + distamycin- A ^c + 2 + MPA	30	74	26
13	DNA + distamycin- A + 6 + MPA	30	70	30
14	DNA + DMSO ^d + 2 + MPA	30	90	10
15	DNA + catalase ^e + 2 + MPA	30	84	16
16	DNA + KI ^f + 2 + MPA	30	86	14
17	DNA + mannitol ^g + 2 + MPA	30	88	12
18	DNA + SOD ^h + 2 + MPA	30	30	70

^a SC and NC are supercoiled and nicked circular forms of DNA. [MPA] = 5 mM.

^b Including ~15–20% linear form.

^c 100 μM.

^d 4 μL.

^e 4 units.

^f 1 mM.

^g 1 mM.

^h 4 units.

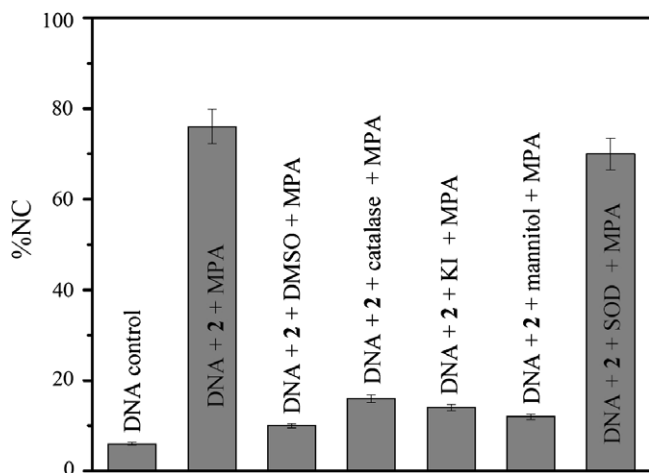
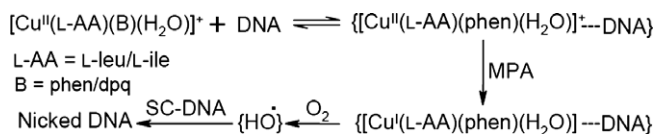


Fig. 8. Cleavage of SC pUC19 DNA (30 μ M) by [Cu(L-leu)(phen)(H₂O)](NO₃) (2) in the presence of MPA (5 mM) with various additives in Tris buffer (pH 7.2) medium. The additive concentrations/quantity are: DMSO (4 μ L), catalase (4 U), KI (1 mM), mannitol (1 mM), SOD (4 U).



Scheme 2. Proposed mechanistic pathway for the chemical nuclease activity of the complexes in Tris-buffer medium.

[50]. The pathways involved in the DNA cleavage reactions are believed to be analogous to those proposed by Sigman and coworkers for the chemical nuclease activity of bis(phen)copper species (Scheme 2) [1,43,44].

4. Conclusions

Ternary redox active copper(II) complexes having N,O-donor α -amino acid L-leucine or L-isoleucine and N,N-donor heterocyclic bases have been prepared and characterized. The copper(II) complexes with planar phenanthroline bases, with a CuN₃O₂ coordination geometry, show efficient DNA binding ability. The phen and dpq complexes were shown to be DNA minor groove binders. The study also confirms that the binding ability of the complexes is an important precondition to show efficient DNA cleavage activity. Efficient chemical nuclease activity is observed for the redox active phen and dpq complexes under physiological reaction conditions via a mechanistic pathway involving formation of hydroxyl radicals in the presence of the reducing agent MPA.

Acknowledgements

The authors gratefully acknowledge the support of Prof. Akhil R. Chakravarty, Department of Inorganic and Physical Chemistry, Indian Institute of Science, Bangalore, India, in providing facilities and useful discussions.

Financial support received from the Department of Science and Technology (DST, SR/S5/BC-14/2006), Government of India, is gratefully acknowledged. R.K. is thankful to DST for a fellowship. A.K.P is thankful to CSIR for a fellowship. Thanks are due to the Alexander von Humboldt Foundation, Germany, for donation of an electroanalytical system; the Convener, Bioinformatics Center, Indian Institute of Science, Bangalore, for a database search; and the DST for the CCD single crystal X-ray diffractometer facility.

Appendix A. Supplementary material

CCDC 662368 and 662369 contain the supplementary crystallographic data for 4 · H₂O and 6. These data can be obtained free of charge via <http://www.ccdc.cam.ac.uk/conts/retrieving.html>, or from the Cambridge Crystallographic Data Centre, 12 Union Road, Cambridge CB2 1EZ, UK; fax: (+44) 1223-336-033; or e-mail: deposit@ccdc.cam.ac.uk. Supplementary data associated with this article can be found, in the online version, at doi:10.1016/j.poly.2007.12.026.

References

- [1] (a) D.S. Sigman, A. Mazumder, D.M. Perrin, *Chem. Rev.* 93 (1993) 2295; (b) D.S. Sigman, *Acc. Chem. Res.* 19 (1986) 180; (c) K.A. Reich, L.E. Marshall, D.R. Graham, D.S. Sigman, *J. Am. Chem. Soc.* 103 (1981) 3582.
- [2] (a) B. Meunier, *Chem. Rev.* 92 (1992) 1411; (b) G. Pratviel, J. Bernadou, B. Meunier, *Adv. Inorg. Chem.* 45 (1998) 251; (c) G. Pratviel, J. Bernadou, B. Meunier, *Angew. Chem., Int. Ed. Engl.* 34 (1995) 746.
- [3] M. Pyle, J.K. Barton, *Prog. Inorg. Chem.* 38 (1990) 413.
- [4] K.E. Erkkila, D.T. Odom, J.K. Barton, *Chem. Rev.* 99 (1999) 2777.
- [5] B. Armitage, *Chem. Rev.* 98 (1998) 1171.
- [6] (a) D.R. McMillin, K.M. McNett, *Chem. Rev.* 98 (1998) 1201; (b) F. Mancin, P. Scrimin, P. Tecilla, U. Tonellato, *Chem. Commun.* (2005) 2540.
- [7] (a) W.K. Pogozelski, T.D. Tullius, *Chem. Rev.* 98 (1998) 1089; (b) T.D. Tullius, J.A. Greenbaum, *Curr. Opin. Chem. Biol.* 9 (2005) 127; (c) E. Boscaglia, M. Gatos, L. Lucatello, F. Mancin, S. Moro, M. Palumbo, C. Sissi, P. Tecilla, U. Tonellato, G. Zagotto, *J. Am. Chem. Soc.* 126 (2004) 4543.
- [8] H.T. Chifotides, K.R. Dunbar, *Acc. Chem. Res.* 38 (2005) 146.
- [9] E.R. Jamieson, S.J. Lippard, *Chem. Rev.* 99 (1999) 2467.
- [10] W.S. Bowen, W.E. Hill, J.S. Lodmell, *Methods Enzymol.* 25 (2001) 344.
- [11] (a) M. Sabat, in: A. Sigel, H. Sigel (Eds.), *Metal ions in Biological Systems*, vol. 32, Marcel Dekker, New York, Basel, 1996; (b) R.N. Mukherjee, *Indian J. Chem.* 42A (2003) 2175.
- [12] (a) A.R. Chakravarty, P.A.N. Reddy, B.K. Santra, A.M. Thomas, *Proc. Ind. Acad. Sci. (Chem. Sci.)* 114 (2002) 391; (b) B.K. Santra, P.A.N. Reddy, G. Neelkanta, S. Mahadevan, M. Nethaji, A.R. Chakravarty, *J. Inorg. Biochem.* 89 (2002) 191; (c) A.M. Thomas, G. Neelkanta, S. Mahadevan, M. Nethaji, A.R. Chakravarty, *Eur. J. Inorg. Chem.* (2002) 2720; (d) A.M. Thomas, M. Nethaji, S. Mahadevan, A.R. Chakravarty, *J. Inorg. Biochem.* 94 (2003) 171; (e) P.A.N. Reddy, M. Nethaji, A.R. Chakravarty, *Eur. J. Inorg. Chem.* (2004) 1440.

- [13] S. Dhar, P.A.N. Reddy, M. Nethaji, S. Mahadevan, M.K. Saha, A.R. Chakravarty, *Inorg. Chem.* 41 (2002) 3469.
- [14] R. Pradhan, A.M. Thomas, A. Mukherjee, S. Dhar, M. Nethaji, A.R. Chakravarty, *Indian J. Chem.* 44A (2005) 18.
- [15] P.U. Maheswari, K. Lappalainen, M. Sfregola, S. Barends, P. Gamez, U. Turpeinen, I. Mutikainen, G.P. van Wezel, J. Reedijk, *J. Chem. Soc., Dalton Trans.* (2007) 3676.
- [16] P.D. Hoog, C. Boldron, P. Gamez, K. S.-Bol, I. Roland, M. Pitie, R. Kiss, B. Meunier, J. Reedijk, *J. Med. Chem.* 50 (2007) 3148.
- [17] (a) A.K. Patra, S. Dhar, M. Nethaji, A.R. Chakravarty, *Chem. Commun.* (2003) 1562;
(b) A.K. Patra, S. Dhar, M. Nethaji, A.R. Chakravarty, *J. Chem. Soc., Dalton Trans.* (2005) 896;
(c) A.K. Patra, M. Nethaji, A.R. Chakravarty, *J. Chem. Soc., Dalton Trans.* (2005) 2798;
(d) A.K. Patra, M. Nethaji, A.R. Chakravarty, *J. Inorg. Biochem.* 101 (2007) 233;
(e) R. Rao, A.K. Patra, P.R. Chetana, *Polyhedron* 26 (2007) 5331.
- [18] H. Li, X.-Y. Le, D.-W. Pang, H. Deng, Z.-H. Xu, Z.-H. Lin, *J. Inorg. Biochem.* 99 (2005) 2240.
- [19] S. Zhang, Y. Zhu, C. Tu, H. Wei, Z. Yang, L. Lin, J. Ding, J. Zhang, Z. Guo, *J. Inorg. Biochem.* 98 (2004) 2099.
- [20] Y. Jin, J. Cowan, *J. Am. Chem. Soc.* 127 (2005) 8408.
- [21] F.V. Pamatong, C.A. Detmer III, R. Bocarsly, *J. Am. Chem. Soc.* 118 (1996) 5339.
- [22] R. Ren, P. Yang, W. Zheng, Z. Hua, *Inorg. Chem.* 39 (2000) 5454.
- [23] A. García-Raso, J.J. Fiol, B. Adrover, V. Moreno, I. Mata, E. Espinosa, E. Molins, *J. Inorg. Biochem.* 95 (2003) 77.
- [24] D.L. Nelson, M.M. Cox, in: *Lehninger, Principles of Biochemistry*, 3rd ed., Worth Publishing, New York, 2000.
- [25] D.D. Perrin, W.L.F. Armarego, D.R. Perrin, *Purification of Laboratory Chemicals*, Pergamon Press, Oxford, UK, 1980.
- [26] E. Amouyal, A. Homsy, J.-C. Chaambron, J.-P. Sauvage, *J. Chem. Soc., Dalton Trans.* (1990) 1841.
- [27] (a) N. Hu, K. Aoki, H. Yamazaki, *Inorg. Chim. Acta* 163 (1989) 105;
(b) X. Le, X. Zhou, C. Huang, X. Feng, *J. Coord. Chem.* 56 (2003) 861;
(c) S. Chen, X. Le, X. Zhou, X. Liu, G. Liu, *Huaxue Tongbao* 67 (2004) 461;
(d) Q. Gu, X.-Y. Le, Y. Xie, L.-F. Hong, C.-X. Zhuang, *Chin. J. Inorg. Chem.* 22 (2006) 757.
- [28] N. Walker, D. Stuart, *Acta Crystallogr.* A39 (1993) 158.
- [29] (a) SMART, Siemens Energy & Automation, Inc., Madison, WI, 1996.;
(b) SAINT Version 4 Software Reference Manual, Siemens Energy & Automation, Inc., Madison, WI, 1996.
- [30] G.M. Sheldrick, *SADABS Version 2 Multi-Scan Absorption Correction Program*, University of Göttingen, Germany, 2001.
- [31] G.M. Sheldrick, *SHELX 97 Programs for Crystal Structure Solution and Refinement*, University of Göttingen, Göttingen, Germany, 1997.
- [32] M.N. Burnett, C.K. Johnson, *ORTEP-III Report ORNL-6895*, Oak Ridge National Laboratory, Oak Ridge, TN, 1996.
- [33] J. Marmur, *J. Mol. Biol.* 3 (1961) 208.
- [34] M.E. Reichmann, S.A. Rice, C.A. Thomas, P. Doty, *J. Am. Chem. Soc.* 76 (1954) 3047.
- [35] A. Wolfe, G.H. Shimer, T. Meehan, *Biochemistry* 26 (1987) 6392.
- [36] (a) J.-B. LePecq, C. Paoletti, *J. Mol. Biol.* 27 (1967) 87;
(b) S. Neidle, *Nat. Prod. Rep.* 18 (2001) 291.
- [37] G. Cohen, H. Eisenberg, *Biopolymers* 8 (1969) 45.
- [38] J. Bernadou, G. Pratiel, F. Bennis, M. Girardet, B. Meunier, *Biochemistry* 28 (1989) 7268.
- [39] A.W. Addison, T.N. Rao, J.V. Reedijk, G.C. Verschoor, *J. Chem. Soc., Dalton Trans.* (1984) 1349.
- [40] J.M. Veal, R.L. Rill, *Biochemistry* 30 (1991) 132.
- [41] J.M. Veal, K. Merchant, R.L. Rill, *Nucleic Acids Res.* 19 (1991) 3383.
- [42] O. Zelenko, J. Gallagher, D.S. Sigman, *Angew. Chem. Int. Ed. Engl.* 36 (1997) 2776.
- [43] D.S. Sigman, *Biochemistry* 29 (1990) 9097.
- [44] J.M. Kelly, A.B. Tossi, D.J. McConnel, C. OhUigin, *Nucleic Acids Res.* 13 (1985) 6017.
- [45] M. Lee, A.L. Rhodes, M.D. Wyatt, S. Forrow, J.A. Hartley, *Biochemistry* 32 (1993) 4237.
- [46] S. Satyanarayana, J.C. Dabrowiak, J.B. Chaires, *Biochemistry* 31 (1992) 9319.
- [47] T. Hirohama, Y. Kuranuki, E. Ebina, T. Sugizaki, H. Arai, M. Chikira, P.T. Selvi, M. Palaniandavar, *J. Inorg. Biochem.* 99 (2005) 1205.
- [48] (a) C. Bailly, J.B. Chaires, *Bioconjugate Chem.* 9 (1998) 513;
(b) M. Coll, C.A. Frederick, A.H.-J. Wang, A. Rich, *Proc. Natl. Acad. Sci. USA* 84 (1987) 8385.
- [49] (a) O.I. Aruoma, B. Halliwell, M. Dizdaroglu, *J. Biol. Chem.* 264 (1989) 13024;
(b) S.M. Klein, G. Cohen, A.I. Cederbaum, *Biochemistry* 20 (1981) 6006.
- [50] S. Inoue, S. Kawanishi, *Cancer Res.* 47 (1987) 6522.